

# ORIENTED SECONDARY STRUCTURE IN INTEGRAL MEMBRANE PROTEINS

## I. Circular Dichroism and Infrared Spectroscopy of Cytochrome Oxidase in Multilamellar Films

MOHAMMED D. BAZZI AND ROBERT W. WOODY

*Department of Biochemistry,*

*Colorado State University,*

*Fort Collins, Colorado 80523*

**ABSTRACT** The circular dichroism (CD) of cytochrome oxidase in solution indicates the presence of both  $\alpha$ -helix ( $\sim 37\%$ ) and  $\beta$ -sheet ( $\sim 18\%$ ). In oriented films generated by the isopotential spin-dry method, the CD measured normal to the film shows a marked decrease in the negative bands at 222 and 208 nm, and a decrease and red shift in the positive band near 195 nm, relative to solution spectra. These features are characteristic of  $\alpha$ -helices oriented with their helix axes along the direction of light propagation. A quantitative estimate of the orientation, based on the ratio of the rotational strengths of the 208-nm band in the film and in solution, leads to an average angle between the helix axis and the normal to the film,  $\phi_\alpha$ , of  $\sim 39^\circ$ . A method for analyzing infrared (IR) linear dichroism is developed that can be applied to proteins with comparable amounts of  $\alpha$ -helix and  $\beta$ -sheet. From analysis of the amide I band,  $\phi_\alpha$  is found to lie between 20 and  $36^\circ$ , depending on the angle that the amide I transition moment forms with the helix axis. A survey of the literature on the amide I transition moment direction indicates that a value of  $\sim 27^\circ$  is appropriate for standard  $\alpha$ -helical systems, such as those in cytochrome oxidase. A larger value, near  $40^\circ$ , is reasonable for systems that have distorted  $\alpha$ -helices, as evidenced by amide I frequencies above  $1,660\text{ cm}^{-1}$ , as is the case of bacteriorhodopsin. This conclusion supports  $\phi_\alpha \sim 36^\circ$  from IR linear dichroism, in agreement with the CD results. Linear dichroism in the amide I and amide II region indicates that the  $\beta$ -sheet in cytochrome oxidase is oriented with the carbonyl groups nearly parallel to the plane of the membrane and the chain direction inclined at  $\sim 40^\circ$  to the normal. Comparison of these results with tentative identification of transmembrane helices from sequence data suggests that either some of the transmembrane helices are inclined at an unexpectedly large angle to the normal, or the number of such helices has been overestimated. Some putative transmembrane helices may be  $\beta$ -strands spanning the membrane.

### INTRODUCTION

Cytochrome oxidase (ferrocytochrome *c*: oxygen oxidoreductase E.C.1.9.3.1) is the terminal component in the respiratory chain in aerobic organisms. The fundamental role of cytochrome oxidase is the four-electron reduction of oxygen, which constitutes the final step in a series of redox reactions that provides the free energy for ATP synthesis. Cytochrome oxidase is a complex enzyme containing two copper atoms, two heme *a* molecules, and a number of subunits, and is an integral membrane protein of the inner mitochondrial membrane. The structural and functional aspects of cytochrome oxidase have been extensively reviewed (1–3).

Three-dimensional crystals of cytochrome oxidase suitable for x-ray diffraction have not been reported, but two-dimensional arrays have been studied by electron microscopy image-reconstruction methods (4, 5). From such analyses, the image of cytochrome oxidase as a Y-shaped molecule inserted asymmetrically in the membrane has emerged. The stalk of the Y is the C domain, protruding from the inner mitochondrial membrane on the cytoplasmic side. The arms of the Y are on the matrix side and are denoted the  $M_1$  and  $M_2$  domains. Low-angle x-ray diffraction experiments on oriented bilayers containing cytochrome oxidase (6) have provided evidence for the presence of a bundle of  $\alpha$ -helices normal to the plane of the membrane.

Although there is still controversy about the exact number of subunits in cytochrome oxidase (7–9), the sequences of all of the subunits that constitute the minimal complex needed for electron transport have been deter-

Dr. Bazzi's address is Dept. of Biochemistry, University of Minnesota, St. Paul, MN 55108.

Correspondence should be addressed to Dr. Woody.

mined (10–12). Structure prediction algorithms have been applied to these sequences and have revealed a number of highly hydrophobic stretches with high helix and/or  $\beta$ -sheet potential (9, 12, 13). A total of 20 such segments has been identified (9) and are proposed to span the lipid bilayer as  $\alpha$ -helices.

In the present study the degree of orientation of the secondary structural elements of cytochrome oxidase is investigated by circular dichroism (CD) and infrared linear dichroism of oriented multilayer films of cytochrome oxidase. These techniques have previously been applied to several integral membrane proteins, namely bacteriorhodopsin (14–16), rhodopsin (17, 18), and various photosynthetic membrane complexes (19–21). All of the above proteins have high  $\alpha$ -helix contents (>50%) and small amounts (<10%) of  $\beta$ -sheet. Cytochrome oxidase has a lower  $\alpha$ -helix content (~35%) and the  $\beta$ -sheet accounts for ~20% of the residues. Therefore,  $\beta$ -sheet contributions to the infrared linear dichroism must be considered. We have extended the linear dichroism analysis to take  $\beta$ -sheets into account, and have obtained information about the orientation of these secondary structural elements as well as the  $\alpha$ -helices.

## MATERIALS AND METHODS

Cytochrome oxidase was isolated from bovine hearts according to the method of Yoshikawa et al. (22). Enzyme concentrations were determined from the difference absorption between reduced and oxidized forms, measured at 605 nm. A value of  $\Delta\epsilon_{605} = 24 \text{ mM}^{-1} \text{ cm}^{-1}$  was used (23). Thin, homogeneous, multilayer films of cytochrome oxidase were produced by the isopotential spin-dry method (24). The films were deposited on quartz coverslips (15 mm diameter, 0.2 mm thickness, ESCO Chemical Co., Oak Ridge, NJ) for the CD measurements, or on AgCl coverslips (cut from 4-mm-thick sheet, Harshaw Chemical Co., Solon, OH) for the infrared dichroism measurements.

## CD Measurements

CD spectra were obtained on a circular dichrograph (model J41C; Japan Spectroscopic Company, Ltd. Tokyo, Japan) interfaced with a minicomputer (Model MINC 11; Digital Equipment Corp., Marlboro, MA). The instrument was calibrated regularly at 290 nm using (+)-camphorsulfonic acid (25). The raw ellipticity values below ~200 nm were low compared with literature values (26), due to improper calibration in this region. The CD of poly ( $\gamma$ -methyl-L-glutamate) in trifluoroethanol measured before and after recalibration was used to calculate a correction factor at each wavelength. With this adjustment, the solution spectra are in excellent agreement with those reported by Myer (26).

Ellipticities are reported as mean residue ellipticities using the average residue molecular weight of 120.5 (26). For film spectra, mean residue ellipticities were calculated from the cross-sectional area of the film and the known amount of sample deposited. The CD spectra were routinely smoothed by the least-squares method of Savitzky and Golay (27), using a cubic polynomial and a 4-nm window. The spectra were resolved into Gaussian components by the damped least-squares method (28).

The quality of the films used for CD was assessed by several tests. The CD spectrum of the film, mounted normal to the beam, was measured. The measurement was repeated after rotating the disk by 90° around the beam direction. The distance of the film from the photomultiplier was also varied. If either of these variations led to significant changes in the observed CD, the film was discarded. Variation with rotation about the normal implies in-plane anisotropy, which can lead to serious linear

dichroism and birefringence artifacts in the CD of films. Variation with distance from the photomultiplier implies differential scattering of left- and right circularly polarized light, another potential source of artifacts in CD (29–31). Observation of apparent CD in the 250–260-nm region was also taken as evidence for either misalignment of the film or, if it could not be eliminated by realignment, of light-scattering artifacts. In the latter case, the film was discarded.

The average orientation of the  $\alpha$ -helical segments was obtained from the ratio of the rotational strengths of the 208-nm band in the film ( $R_f$ ) and in solution ( $R_s$ ). The orientation was calculated using the following equation, derived in the Appendix:

$$\sin^2 \phi_a = 2 R_f / (3 R_s), \quad (1)$$

where  $\phi_a$  is the average angle between the helix axes and the normal to the film. It should be noted that the use of resolved rotational strengths, while subject to some uncertainty, eliminates the contributions of other CD bands from the  $\alpha$ -helix or other conformations. The ratio of observed ellipticities at 208 nm, while determinable with higher accuracy, would be subject to other contributions.

Secondary structural estimates were performed by an unconstrained least-squares method. The basis spectra of Bolotina et al. (32, 33), Chang et al. (34), and Hennessey and Johnson (35) were used. In addition, the CD spectra of 16 proteins (34) were used directly as a basis set according to the method of Provencher and Glockner (36), or were first transformed to an orthogonal basis set by the method of Hennessey and Johnson (35). The basis spectra were obtained from the original papers (32, 33, 35) or supplied by the authors (34). The protein CD spectra of Chang et al. (34) were obtained as part of the program CONTIN (36). Each method was applied to sixteen independently determined CD spectra. To be acceptable, the final solutions were required to have positive values for all fractional contents of secondary structural elements, and these fractional values summed to a value between 0.8 and 1.2. A ridge regression method (36, 37), with constraints of non-negative fractions and a unit sum, was also applied to the data with results which differed only slightly from those obtained from least-squares analysis.

## IR Measurements

All IR measurements were performed on a spectrophotometer (model 580; Perkin-Elmer Corp., Norwalk, CT) or a model 180 (Perkin-Elmer Corp.) equipped with an AgBr polarizer. Solution studies were performed on D<sub>2</sub>O-exchanged samples, with D<sub>2</sub>O as the solvent. D<sub>2</sub>O exchange was accomplished by four cycles of dilution of a concentrated sample, initially in H<sub>2</sub>O, with 99.8% D<sub>2</sub>O (Sigma Chemical Co., St. Louis, MO), in alternation with concentration by ultrafiltration XM50 filter (Amicon Corp., Danvers, MA).

Linear dichroism measurements were carried out on a film that was tilted so that its normal made an angle of 60° with the sample beam. Horizontally polarized radiation was polarized parallel to the plane of the film, while vertically polarized radiation was polarized at an angle of 60°, with respect to the plane of the film.

The following equation, derived in the Appendix, was used to determine the orientations of the helix and  $\beta$ -sheet:

$$R - 1 = 3 \frac{\sin^2 \theta_0}{n^2} \frac{f_\alpha \epsilon'_\alpha S'_\alpha + f_\beta \epsilon'_\beta S'_\beta}{f_\alpha \epsilon'_\alpha (1 - S'_\alpha) + f_\beta \epsilon'_\beta (1 - S'_\beta) + f_u}. \quad (2)$$

The meaning of the various terms in this equation is as follows:

$R$	observed dichroic ratio at a given frequency, $A_V/A_H$ , where $A_V$ is the absorbance for vertically polarized light and $A_H$ is the absorbance for horizontally polarized light
$\theta_0$	the angle through which the film is tilted
$n$	refractive index of the film
$f_\alpha, f_\beta, f_u$	fraction of residues in $\alpha$ -helix, $\beta$ -sheet, and unordered conformation, respectively
$\epsilon'_\alpha, \epsilon'_\beta$	relative extinction coefficients of $\alpha$ -helix and $\beta$ -sheet at the

frequency in question, defined as the ratios ( $\epsilon_a/\epsilon_u$ ), and ( $\epsilon_\beta/\epsilon_u$ ), respectively, where  $\epsilon_u$  is the molar extinction coefficient of the unordered form.

$S'_\alpha$ ,  $S'_\beta$  order parameters for  $\alpha$ -helix and  $\beta$ -sheet, respectively.

Measurements of the dichroic ratio at two different frequencies permit both order parameters to be determined using Eq. 2. The fractions  $f_\alpha$ ,  $f_\beta$ , and  $f_u$  were obtained from analysis of the CD spectrum, assuming that  $f_u = 1 - f_\alpha - f_\beta$ . The  $\beta$ -turn contributions are assumed to be isotropic and equivalent to the unordered conformation. The relative extinction coefficients were calculated assuming that the absorption spectra for the three conformational types are Lorentzian bands with identical half widths and peak heights, differing in band position. For the amide I band, the half width was assumed to be  $20 \text{ cm}^{-1}$ , based upon the spectra of model polypeptides (38). The  $\alpha$ -helix and unordered conformations were taken to have their amide I band at  $1,655 \text{ cm}^{-1}$  and the  $\beta$ -sheet at  $1,630 \text{ cm}^{-1}$ . The amide II band half width was assumed to be  $30 \text{ cm}^{-1}$ , with  $\nu_\alpha = 1,545 \text{ cm}^{-1}$ ,  $\nu_\beta = 1,530 \text{ cm}^{-1}$ , and  $\nu_u = 1,535 \text{ cm}^{-1}$ . It should be noted that in previous analyses of proteins containing only  $\alpha$ -helix and unordered conformations (15–21), it has been assumed that the molar extinction coefficient per residue is the same for the  $\alpha$ -helix and the unordered conformation, i.e.,  $\epsilon'_\alpha = 1$ . This is probably a reasonable approximation in the case of the amide I band, for which the  $\alpha$ -helix and unordered conformations have very similar peak frequencies, near  $1,655 \text{ cm}^{-1}$ . It is less reasonable for the amide II band, where the frequencies of maximum absorbances of the  $\alpha$ -helix and unordered form differ by  $\sim 10 \text{ cm}^{-1}$ . It is not acceptable to assume that  $\epsilon'_\beta = 1$ , except at a single isosbestic frequency that is unlikely to be useful in analysis.

The order parameter of the  $\alpha$ -helix is related to the average angle between the helix axes and the normal to the film through the equation (15, 39)

$$S'_\alpha = S_{ms} S_{\alpha M} S_\alpha \quad (3)$$

$S_{ms}$  is the order parameter for the mosaic spread, resulting from incomplete orientation of the membrane fragments. We take  $S_{ms} = 1$ , since measurements of this parameters for films formed by this (24, 40) or similar (41) techniques generally gives  $S_{ms} > 0.9$ . To the extent that the membrane orientation is less than perfect, the angles of deviation of the  $\alpha$ -helix and  $\beta$ -sheet axes from the normal will be overestimated.

The parameter  $S_{\alpha M}$  is related to the angle between the transition moment and the helix axis,  $\phi_{\alpha M}$ , where  $M$  denotes the amide transition (I or II):

$$S_{\alpha M} = (3 \cos^2 \phi_{\alpha M} - 1)/2 \quad (4)$$

For the  $\alpha$ -helix, two rather discordant values of  $\phi_{\alpha I}$  have been reported for the amide I transition,  $39^\circ$  (42) and  $27.6^\circ$  (43). These correspond to  $S_{\alpha I} = 0.406$  and  $S_{\alpha I} = 0.678$ , respectively. For the amide II band, the values of  $\phi_{\alpha II}$  are  $75^\circ$  (42) or  $75.3^\circ$  (43), corresponding to  $S_{\alpha II}$  of  $-0.400$  and  $-0.403$ , respectively.

The final factor in  $S'_\alpha$  is the one in which we are interested, namely the parameter describing the average orientation of the helix axes.  $S_\alpha$  is related to the angle  $\phi_\alpha$ , the average angle between the helix axis and the normal to the membrane, by

$$S_\alpha = (3 \cos^2 \phi_\alpha - 1)/2 \quad (5)$$

The observed order parameter for the  $\beta$ -sheet can be related to the same type of parameters:

$$S'_\beta = S_{ms} S_{\beta M} S_\beta \quad (6)$$

Here, however,  $S_{\beta M}$  is simpler because in the  $\beta$ -sheet, the amide I transition is split into two (in parallel sheets) or three (antiparallel sheets) components. The strongest component is near  $1,630 \text{ cm}^{-1}$ , and is polarized in the plane of the sheet along the hydrogen-bond direction (perpendicular to the chain direction). The weakness of the other components and

the large splitting leads to the conclusion that for the amide I band  $S_{\beta I} = 1$ , and the angle  $\phi_{\beta I}$  will reflect the angle between the membrane normal and the H-bond direction. A similar argument holds for the amide II, with the angle  $\phi_{\beta II}$  reflecting the angle between the membrane normal and the chain direction. In contrast to the  $\alpha$ -helix, two angles are needed to specify the orientation of the  $\beta$ -sheet. These can be obtained, at least approximately, from the present analysis.

## RESULTS

### Circular Dichroism

The far-ultraviolet CD spectrum of cytochrome oxidase is shown in Fig. 1. The spectrum is in excellent agreement with that reported by Myer (26). The spectrum is characteristic of a protein with a significant amount of  $\alpha$ -helix, with negative maxima at 220 and 208 nm. The positive maximum of 195 nm is red-shifted from the usual  $\alpha$ -helix peak near 192 nm. This shift was noted by Myer (26), who attributed it to the presence of  $\beta$ -sheet.

The CD spectrum of cytochrome oxidase, measured with light incident normal to the plane of oriented cytochrome oxidase films, is shown in Fig. 1. Comparison with the solution spectrum shows several qualitative differences: in the spectrum of the film the 220-nm band is weaker, the 208-nm band is markedly diminished, and the 195 nm-band is further red-shifted and decreased in magnitude. These features of the oriented sample are all qualitatively consistent with those expected (44, 45) and observed (14, 17, 46) for a system of  $\alpha$ -helices whose axes are oriented predominantly parallel to the direction of light propagation.

The CD spectra in Fig. 1 have been analyzed as a sum of Gaussians, assuming either three or four components (Table I). The three-band analysis gave a reasonably good fit to both spectra in terms of root-mean-square (RMS) error ( $\sim 1.5\%$ ). However, the band positions and band widths required to fit the solution and film spectra differ significantly. When four Gaussian bands are used, the RMS error is about half as large and the band parameters

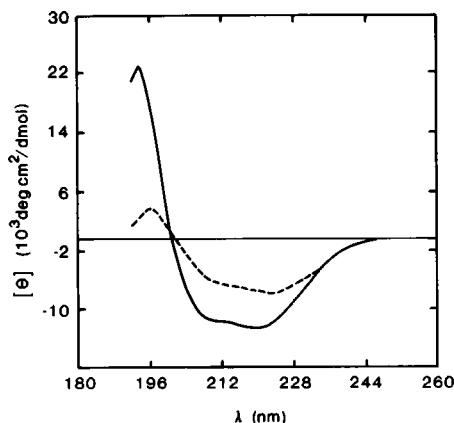


FIGURE 1 CD spectra of cytochrome oxidase in solution (—) and in oriented membrane films (-----).

TABLE I  
BAND PARAMETERS FROM THE GAUSSIAN  
DECONVOLUTION OF THE CD SPECTRA OF  
CYTOCHROME OXIDASE

Sample	No. of bands	RMS error	$[\theta]_{\max}$	Position	Width*	R
		%	deg cm <sup>2</sup> /dmol	nm	nm	DBM <sup>†</sup>
Film	3	1.5	-5,744	226.63	11.48	-0.0388
			-4,562	212.13	12.39	-0.0354
			5,005	197.41	5.53	+0.0185
Solution	3	1.6	-12,239	220.21	13.14	-0.0968
			-5,718	207.53	5.48	-0.0201
			22,977	194.52	4.88	+0.0765
Film	4	0.9	-6,536	225.78	11.77	-0.0452
			-2,524	216.31	7.53	-0.0116
			-3,010	208.44	6.19	-0.0119
			4,169	196.93	4.73	+0.0133
Solution	4	0.7	-11,105	221.68	12.31	-0.0817
			-2,691	211.92	9.34	-0.0157
			-5,468	207.07	5.70	-0.0200
			23,109	194.18	5.30	+0.0837

\*Half of the band width at  $e^{-1} \times$  maximum amplitude.

<sup>†</sup>1 DBM = 1 debye-bohr magneton =  $0.9273 \times 10^{-38}$  cgs unit.

(other than amplitude) show much better agreement between solution and film.

From Table I it can be seen that the 220-nm band, attributable to the  $\alpha$ -helix  $n\pi^*$  transition, is only about half as strong in the film as in solution. The second band is located at 216 nm in the film spectrum and at 212 nm in the solution spectrum. This band can be assigned to the  $\beta$ -sheet, for which there is evidence from both CD and IR (see below). The  $\beta$ -sheet is characterized by having an  $n\pi^*$  CD band near 216–217 nm. The discrepancy between the wavelengths for the solution and the film is probably due largely to the difficulty of precisely locating this band, which is overlapped on each side by bands of the same sign

and, unlike the other bands, does not correspond to an extremum or inflection in the raw spectrum.

A quantitative estimate of the  $\alpha$ -helix orientation can be obtained from the rotational strengths of the 207–208-nm bands in the film and solution spectra. Substitution of these values from Table I in Eq. 1 gives a value of  $\phi_\alpha = 39^\circ$ , i.e., the helix axes are, on the average, oriented at an angle of  $39^\circ$  from the normal to the membrane.

The solution CD spectrum of cytochrome oxidase in Fig. 1 was also used to obtain information about the secondary structure content of the protein. The results from various methods of analysis are presented in Table II. The different methods give estimates for the  $\alpha$ -helix content that are consistently near the mean of 37%. Although the  $\beta$ -sheet estimates show larger variations, the mean value of 18% is a reliable indicator that a significant amount of  $\beta$ -sheet is present in cytochrome oxidase. The estimates of  $\beta$ -turn and unordered conformation are individually less reliable than is their sum.

**Infrared.** The IR spectrum of cytochrome oxidase in D<sub>2</sub>O solution is shown in Fig. 2. The bands at 1,736 and 1,655 cm<sup>-1</sup> are due to the ester carbonyl stretch of bound lipids and the amide I band of the protein, respectively. The position of the amide I band at 1,655 cm<sup>-1</sup> suggests that the  $\alpha$ -helix is the dominant type of regular secondary structure in cytochrome oxidase, in agreement with the CD results. The amide I band has shoulders at 1,685 and 1,633 cm<sup>-1</sup>, which are consistent with the presence of antiparallel  $\beta$ -sheet, but these features also may have contributions from  $\beta$ -turns (47, 48). The bands at 1,547 and 1,458 cm<sup>-1</sup> are the amide II bands of nondeuterated and deuterated peptide groups, respectively. The frequency of the amide II, 1,547 cm<sup>-1</sup>, is further evidence for the presence of  $\alpha$ -helical regions, which exchange slowly with solvent.

The degree of orientation of secondary structure in

TABLE II  
ACCEPTABLE\* ESTIMATES OF THE SECONDARY STRUCTURE OF CYTOCHROME OXIDASE AS DETERMINED  
BY THE UNCONSTRAINED LEAST-SQUARES METHOD

Method	Ref.	$n^\dagger$	Helix	$\beta$ -Sheet	$\beta$ -Turn	Others	Sum
			%	%	%	%	%
Bolotina	32	3	39.6 $\pm$ 6.8 <sup>‡</sup>	11.4 $\pm$ 0.9 <sup>‡</sup>	12.0 $\pm$ 4.2 <sup>‡</sup>	32.5 $\pm$ 1.8 <sup>‡</sup>	95.5
Bolotina	33	4	38.9 $\pm$ 6.2	17.1 $\pm$ 3.2	13.6 $\pm$ 2.6	31.3 $\pm$ 5.3	100.9
Chang	34	10	36.6 $\pm$ 6.9	19.4 $\pm$ 13.5	10.4 $\pm$ 7.7	27.4 $\pm$ 6.0	93.8
Hennessey	35	7	38.5 $\pm$ 6.1	19.2 $\pm$ 4.9	16.9 $\pm$ 2.9	23.5 $\pm$ 3.2	98.1
Vectors	<sup>†</sup>	8	35.7 $\pm$ 1.2	22.4 $\pm$ 2.9	19.2 $\pm$ 1.2	30.3 $\pm$ 2.0	107.6
Provencher	36 <sup>†</sup>	6	31.7 $\pm$ 4.2	16.7 $\pm$ 12.3	9.0 $\pm$ 8.0	35.1 $\pm$ 4.5	92.5 <sup>‡</sup>
Averages			36.8 $\pm$ 2.9	17.7 $\pm$ 3.7	13.5 $\pm$ 3.9	30.0 $\pm$ 4.1	98.0

\*The solution of the unconstrained least-squares method was acceptable if the sum of the fraction was between 0.8 to 1.20, and none of the fractions were negative.

<sup>†</sup>The number of acceptable solutions (out of total of 16 trials).

<sup>‡</sup>Standard deviation.

<sup>†</sup>Method of Hennessey and Johnson (35) applied to the CD data of Chang et al. (34) for 16 proteins (see text).

<sup>†</sup>Method of Provencher and Glöckner with constraints of non-negative fractions and unit sum removed.

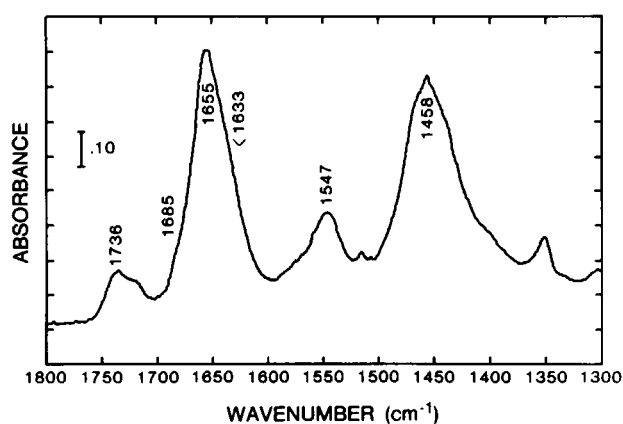


FIGURE 2 IR spectra of cytochrome oxidase in  $D_2O$  solution. Each division on the ordinate scale is 0.10 absorbance unit.

cytochrome oxidase was studied by polarized IR spectroscopy on films. The linear dichroism spectrum of cytochrome oxidase is shown in Fig. 3. In the amide I region, the linear dichroism spectrum has a positive maximum at  $1,662\text{ cm}^{-1}$ , and a negative maximum at  $1,639\text{ cm}^{-1}$ . The amide II region has a single, rather weak, negative band at  $\sim 1,545\text{ cm}^{-1}$ .

Qualitatively, the positive  $1,662\text{ cm}^{-1}$  dichroism indicates preferential orientation of the  $\alpha$ -helices, with their axes normal to the film, while the negative  $1,639\text{ cm}^{-1}$  band suggests that the  $\beta$ -sheets are oriented with their C=O bonds predominantly parallel to the film. The negative dichroism in the amide II region is consistent with the orientation for the  $\alpha$ -helix axes inferred from CD and the amide I dichroism, but the weakness of the amide II dichroism band suggests that the  $\beta$ -sheet contribution is either weakly negative or perhaps positive. This, in turn,

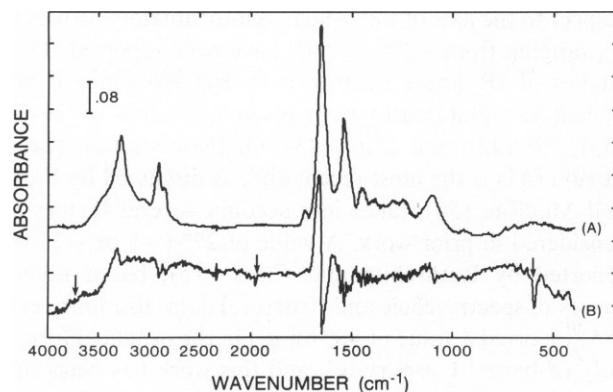


FIGURE 3 Polarized IR spectra of cytochrome oxidase in oriented membrane films. Curve A is the spectrum taken with horizontally polarized light, with the electric vector parallel to the plane of the membrane. Curve B is the difference between the absorbance of vertically and horizontally polarized light,  $A_v - A_h$ . The plane of the film has been tilted so that the electric vector of vertically polarized light is incident at an angle of  $60^\circ$  to the plane of the film. The difference curve has been multiplied by a factor of 5. Each division on the ordinate scale corresponds to 0.08 absorbance unit. The features in spectrum B marked by vertical arrows result from instrumental artifacts.

TABLE III  
INFRARED LINEAR DICHROISM OF  
CYTOCHROME OXIDASE FILMS

	Amide I		Amide II
$\nu_{\max} (\text{cm}^{-1})^*$	1,662	1,639	1,545
R	1.142	0.898	0.965

\*Frequency of extremum in the linear dichroism spectrum,  $A_v - A_h$ .

argues against the plane of the  $\beta$ -sheet being parallel to the plane of the film, as the amide II dichroism of the  $\beta$ -sheet would be strongly negative for such an orientation.

Quantitative analysis of the dichroism data (Table III) was carried out using Eqs. 2–6, and the results are summarized in Table IV. Because the amide II dichroism was relatively weak and the spectrum in that region had a rather high noise level, no attempt was made to extract an independent estimate of the  $\alpha$ -helix orientation. Instead, the value obtained from the amide I region was used to predict the order parameter  $S'_\alpha$  for this region, and only  $S'_\beta$  was determined from the data. The  $S_{\alpha I}$  and  $S_{\alpha II}$  values for the  $\alpha$ -helix drawn from both Tsuboi (42) and Suzuki (43) were used in the analysis. The refractive index of the film was generally assumed to be 1.5 (16). However, some calculations were performed with the value of 1.7 recommended by Rothschild and Clark (15), as well as the lower value of 1.4.

Infrared linear dichroism indicates that  $\phi_\alpha$  is either  $36^\circ$  or  $20^\circ$ , depending on which amide I transition moment directions are assumed. The value obtained with the Suzuki (43) parameters,  $36^\circ$ , is in good agreement with the value of  $39^\circ$  obtained from CD, while the Tsuboi (42) parameters indicate a considerably higher degree of order of the  $\alpha$ -helix axes. If a larger value of refractive index (1.7) is used, the Suzuki parameters yield  $\phi_\alpha = 30^\circ$ , while

TABLE IV  
ANALYSIS OF LINEAR DICHROISM SPECTRA

$f_\alpha$	$f_\beta$	$n$	Transition moments*	$\phi_\alpha^\dagger$	$\phi_{\beta I}^\ddagger$	$\phi_{\beta II}^\ddagger$
0.368	0.177	1.5	S	36	(90)	35
			T	20	(90)	(0)
0.368	0.177	1.7	S	30	(90)	29
			T	(0)	(90)	(0)
0.368	0.177	1.4	S	38	(90)	37
			T	26	(90)	14
0.368	0.260	1.5	S	37	89	43
			T	24	89	29
0.368	0.226	1.4	S	37	90	40
			T	27	90	28

\*S indicates that the Suzuki (43) transition moment directions were used for the  $\alpha$ -helix and T indicates the Tsuboi (42) parameters.

$^\dagger$ A value of zero in parentheses indicates that the order parameter was calculated to be  $>1$ .

$^\ddagger$ A value of 90 in parentheses indicates that the order parameter was calculated to be  $<-0.5$ .

the Tsuboi parameters give  $S > 1$ , a physically impossible value. The  $\alpha$ -helix content was allowed to vary by one standard deviation ( $\pm 2.9\%$ ) about the mean (Table II), keeping other parameters fixed. This led to variations of  $\sim \pm 2^\circ$  in the  $\phi_\alpha$  values, with the larger helix content giving a lower degree of order.

Analysis of the amide I region yields a value of  $S'_{\beta I}$ , which is more negative than  $-0.5$ , the lower limit of the order parameter. This physically impossible result presumably reflects a combination of experimental error and uncertainties in the parameters used in the analysis. It is consistent with our qualitative interpretation of the dichroism data, indicating that  $\phi_{\beta I} \sim 90^\circ$ . Exploration of the effects of varying  $n$  and  $f_\beta$  showed that higher values of  $n$  exacerbate the problem, while higher values of  $f_\beta$  make  $S'_{\beta I}$  more positive. To bring  $S'_{\beta I}$  to an acceptable value of  $-0.5$ ,  $n$  would have to be reduced to an unlikely value of  $< 1.3$ . If  $f_\beta$  is increased to  $0.26$  (with  $n = 1.5$  and  $f_\alpha = 0.368$ ),  $S'_{\beta I} = 0.49$ . This change in  $f_\beta$  has only a minor effect on  $\phi_\alpha$ , increasing it to  $37^\circ$  for the Suzuki parameters and  $24^\circ$  for the Tsuboi parameters. Given the quantitative uncertainties in determining  $\beta$ -sheet content by CD, this is a reasonable resolution of the problem but not a unique one. In any event, the results clearly point to the conclusion that the  $\beta$ -sheets in cytochrome oxidase are oriented such that their carbonyl groups are nearly parallel to the plane of the membrane.

Analysis of the amide II region utilized the value of  $\phi_\alpha$  determined from the amide I linear dichroism. The two alternative values of  $\phi_\alpha$  yield different values of  $\phi_{\beta II}$ . The Suzuki (43) parameters give a value for  $\phi_{\beta II}$  of  $35^\circ$ , while the Tsuboi (42) transition moment directions yield a value of  $S'_{\beta II}$  greater than one. If  $f_\beta$  is taken to be  $0.26$  rather than  $0.177$ , the  $\phi_{\beta II}$  value become  $43^\circ$  (Suzuki) or  $29^\circ$  (Tsuboi). Thus, the assumption of a larger  $\beta$ -sheet content helps resolve this difficulty also. The overall conclusion is that the  $\beta$ -sheets are oriented so that the chain directions are more nearly normal to the plane than in the plane.

## DISCUSSION

CD spectroscopy on solutions of cytochrome oxidase reveals that  $\sim 37\%$  of the protein is in  $\alpha$ -helices. This estimate is in good agreement with the value obtained by Myer (26) from the amplitude of the  $222\text{-nm}$  band ( $39\%$  for oxidized and  $44\%$  for reduced cytochrome oxidase). Myer also obtained a much lower estimate ( $\sim 15\%$ ) from the method of isodichroic points (49), but this method gave an unrealistically large  $\beta$ -sheet content ( $\sim 60\%$ ), and cannot be considered reliable. We estimate  $\beta$ -sheet content at  $\sim 18\%$  from the solution CD, but the linear dichroism analysis suggests that a somewhat higher value,  $\sim 25\text{--}30\%$ , may be more appropriate. CD estimates of  $\beta$ -sheet content are subject to considerably larger error than for  $\alpha$ -helix. Capaldi (50) presented infrared evidence for  $\alpha$ -helix and  $\beta$ -sheet in cytochrome oxidase. He estimated an upper

limit of  $59\%$  for the  $\alpha$  and  $\beta$  content, based on the fraction of slowly exchanging protons.

Measurements of CD on the oriented films give an average angle of  $39^\circ$  for the inclination of the helix axis to the membrane normal. This is the first case in which the oriented CD has been applied to a quantitative analysis of helix orientation. Muccio and Cassim (14), who pioneered the qualitative application, stated that "complexities due to quadrupole moment contributions and changes in effective electromagnetic field due to indices of refraction prevent quantitative correlation of the solution and film spectra." However, Eq. 1 is correct regardless of the mechanism that generates the rotational strength of the  $208\text{-nm}$  band. Therefore, quadrupole effects are irrelevant if valid estimates of the rotational strength of this band can be made in both solution and film. The effective field argument is questionable because the peptide backbone in protein  $\alpha$ -helices is effectively shielded from solvent by the side chains. For example, it has been shown (51) that poly( $\gamma$ -dodecyl-L-glutamate) has, within experimental error, identical CD spectra in hexane, dodecane, and cyclohexane, with refractive indices ranging from  $1.38$  to  $1.43$ . Moreover, the ellipticity values do not differ significantly from those for poly(Glu) or poly(Lys) in water ( $n = 1.33$ ), or for poly (GluOMe) in hexa-fluoroisopropanol ( $n = 1.28$ ) (52).

Comparison of rotational strengths of the parallel-polarized band of the  $\alpha$ -helix at  $208\text{ nm}$  in solution and in films should, therefore, provide a valid measure of the degree of orientation. The principal sources of error, other than experimental errors, are the uncertainties inherent in Gaussian decompositions.

Quantitative interpretation of the IR linear dichroism measurements requires information about the orientation of the amide I and II transition dipole moments, with respect to the axis of the  $\alpha$ -helix. Unfortunately, values for  $\phi_{\alpha I}$  ranging from  $\sim 27^\circ$  to  $\sim 40^\circ$  have been reported. Three studies of IR linear dichroism in oriented films of poly( $\gamma$ -benzyl-L-glutamate) have given  $\phi_{\alpha I}$  values of  $29\text{--}34^\circ$  (53),  $39^\circ$  (42), and  $27.6^\circ$  (43). Of these studies, that of Suzuki (43) is the most recent and, as discussed by Fraser and MacRae (54), takes into account several factors not considered in prior work. A value of  $27^\circ$  ( $+5$  or  $-7$ ) was reported by Rothschild and Clark (15), based upon a survey of spectroscopic and structural data. Bradbury et al. (55) reported a value of  $40^\circ$  for  $\phi_{\alpha I}$  in the  $\alpha$ -helical form of poly( $\beta$ -benzyl-L-aspartate), and this work has been cited as evidence for a larger value for this angle. However, the amide I frequency of this polypeptide,  $1,664\text{ cm}^{-1}$ , is anomalously high, and indicates that the conformation differs from that of most  $\alpha$ -helical polypeptides.

For cytochrome oxidase, the lower value of  $\phi_{\alpha I}$  gives an average helix orientation in good agreement with that obtained from CD. In nearly all previous IR dichroism investigations of integral membrane proteins (15–21), however, a higher value of  $\phi_{\alpha I}$  has been used. In the case of

bacteriorhodopsin, the value of  $\phi_{al} = 39^\circ$  gives an average angle of  $9^\circ$  for the helix axis orientation (16), in good agreement with the three-dimensional Fourier map from electron diffraction (56, 57). If  $\phi_{al} = 27^\circ$ , the amide I dichroism of bacteriorhodopsin (16) would imply an angle  $\phi_\alpha = 32^\circ$ . The amide I frequency of bacteriorhodopsin is considerably higher than that of most  $\alpha$ -helical polypeptides—1,665  $\text{cm}^{-1}$  (58) vs. 1,650–1,655  $\text{cm}^{-1}$  (42, 53, 54). This suggests a distorted  $\alpha$ -helical structure, with hydrogen bonds longer than in the normal  $\alpha$ -helix (58). Krimm and Dwivedi (59) have shown that an  $\alpha_{II}$ -helix (60) is consistent with the unusual features observed in both the amide I and II regions of bacteriorhodopsin. The  $\alpha_{II}$ -helix has the same number of residues per turn and rise per residue as the conventional  $\alpha$ -helix ( $\alpha_I$ ), but a different set of  $\phi$  and  $\psi$  values. In particular, the peptide plane is more strongly tilted, with the carbonyl oxygen oriented away from the helix axis. Krimm and Dwivedi (59) point out that the  $\alpha_{II}$  helix will have a larger perpendicular component of the amide I transition moment, i.e.,  $\phi_{al}$  will be larger.

Therefore, for normal  $\alpha$ -helices, the Suzuki (43) parameters appear to be most suitable. For  $\alpha$ -helices with distortions leading to higher amide I frequencies above  $\sim 1,660 \text{ cm}^{-1}$ , the amide I transition moment is more strongly inclined with respect to the axis. For such systems (bacteriorhodopsin [58], poly- $\beta$ -benzyl-L-aspartate [55]), the Tsu-boi (42) parameters are more appropriate. In cytochrome oxidase, the peak amide I frequency is 1,655  $\text{cm}^{-1}$ , suggesting that the  $\alpha$ -helices have a normal conformation. Therefore, the Suzuki (43) parameters are to be preferred in the IR dichroism analysis.

The  $\beta$ -sheet in cytochrome oxidase is oriented such that the carbonyl groups are essentially parallel to the plane, and the chains are tilted at an angle of  $\sim 40^\circ$  relative to the normal. This is the first membrane protein for which information about the orientation of  $\beta$ -sheets has been deduced from IR linear dichroism.

It is of interest to consider these data on secondary structure content and orientation in the light of other structural information on cytochrome oxidase. From an analysis of the sequences of the various subunits, Capaldi and co-workers (3) have located 21 segments with hydrophobic side chains that they consider to be candidates for transmembrane helices. Assuming that each segment is at least 20 residues long, such transmembrane helices would account for at least 30% of the  $\sim 1,400$  residues in a cytochrome oxidase monomer (166 kD). Since the total helix content is  $\sim 37\%$ , this leaves only 100  $\alpha$ -helical residues in the substantial fraction of the molecule external to the membrane. It is anticipated that  $\alpha$ -helical segments spanning the membrane will have their axes aligned fairly closely to the normal, as in bacteriorhodopsin, in which the helical segments are at most  $20^\circ$  from the normal (56, 57). The observation of  $\phi_\alpha \sim 40^\circ$  is difficult to reconcile with such a picture. If 400 residues were in transmembrane

helices, the helix axes of which were tilted by  $\sim 10^\circ$  from the normal, and all helices with the 100 remaining residues were at  $90^\circ$ , the average angle would only be  $28^\circ$ , barely compatible with the lowest angle estimated from IR dichroism. If the transmembrane helices were tilted at  $20^\circ$ , the overall average would only increase to  $33^\circ$ .

Therefore, our results suggest that if there are of the order of 20 transmembrane helices in cytochrome oxidase, some of them must deviate substantially from a normal orientations. Alternatively, some of the highly hydrophobic stretches identified by Capaldi et al. (3) may be buried  $\alpha$ -helices in domains external to the membrane, or may be strands of  $\beta$ -sheet penetrating the membrane. The preferred orientation of  $\beta$ -sheet that we have found in cytochrome oxidase is consistent with a significant number of  $\beta$ -strands running approximately normal to the membrane. There are no established cases of  $\beta$ -strands spanning biological membranes, but  $\beta$ -sheet has been reported in gap junctions (61) and in porin (62). Furthermore, Jap et al. (63) have suggested that three of the features in the electron diffraction map of bacteriorhodopsin that have been interpreted as slewed  $\alpha$ -helices (56) may in fact be  $\beta$ -strands. The role of  $\beta$ -sheets in integral membrane proteins remains to be established.

## APPENDIX

### Derivation of Eq. 1

Let  $R_z$  be the rotational strength of the 208-nm band measured in solution. This is related to the rotational strengths for the band measured in the  $x$ -,  $y$ -, and  $z$ -directions, denoted by  $R_{xx}$ ,  $R_{yy}$ , and  $R_{zz}$ , respectively.

$$R_z = (R_{xx} + R_{yy} + R_{zz})/3. \quad (\text{A1})$$

Since the 208-nm band is polarized along the helix, i.e., the  $z$ -direction,  $R_{zz} = 0$ , and by helical symmetry,  $R_{xx} = R_{yy} = R_\perp$ . Therefore,

$$R_z = 2R_{xx}/3 = 2R_\perp/3. \quad (\text{A2})$$

In the film, the rotational strength of the 208-nm band,  $R_f$ , is given by:

$$R_f = R_\perp \sin^2 \phi_\alpha + R_{zz} \cos^2 \phi_\alpha, \quad (\text{A3})$$

where  $\phi_\alpha$  is the angle between the helix axis and the direction of observation, normal to the film. Therefore, for the 208-nm band we have

$$R_f/R_z = R_\perp \sin^2 \phi / (2R_\perp/3) = 3 \sin^2 \phi_\alpha/2 \quad (\text{A4})$$

and so

$$\sin^2 \phi_\alpha = 2R_f/(3R_z). \quad (\text{A5})$$

### Derivation of Eq. 2

The following derivation is based upon that of Rothschild et al. (18), generalized to include contributions of  $\beta$ -sheets. The dichroic ratio,  $R$ , at a given frequency is defined by

$$R = A_v/A_h, \quad (\text{A6})$$

where  $A_h$  is the absorption for light polarized horizontally, i.e., parallel to the plane of the film, and  $A_v$  is the absorption for light polarized

vertically. In the film, this polarization direction is at an angle  $\theta$ , such that

$$\sin \theta = \sin \theta_0 / n, \quad (\text{A7})$$

where  $n$  is the refractive index of the film and  $\theta_0$  is the angle through which the film is tilted about the horizontal axis from the plane normal to the beam.

If the protein contained a single type of secondary structure, the order parameter  $S_i$  for that structure could be obtained from the dichroic ratio through the equation (15):

$$R = 1 + 3S_i \sin^2 \theta / (1 - S_i). \quad (\text{A8})$$

In general, the protein will contain  $\alpha$ -helix,  $\beta$ -sheet,  $\beta$ -turns, and unordered conformations. We shall assume that the latter two contributions are isotropic, and focus on the anisotropy due to the  $\alpha$ -helix and  $\beta$ -sheet. We define dichroic ratios for the  $\alpha$ -helix and  $\beta$ -sheet as follows:

$$R'_\alpha = (A_\alpha)_V / (A_\alpha)_H = 1 + 3S'_\alpha \sin^2 \theta / (1 - S'_\alpha) \quad (\text{A9})$$

$$R'_\beta = (A_\beta)_V / (A_\beta)_H = 1 + 3S'_\beta \sin^2 \theta / (1 - S'_\beta). \quad (\text{A10})$$

These dichroic ratios are those that would be observed if we could measure only the contributions of the  $\alpha$ -helix or  $\beta$ -sheet. They are related to the order parameters,  $S'_\alpha$  and  $S'_\beta$ , respectively, through Eqs. A9 and A10, which are the quantities that are to be determined.

The absorbance for horizontally polarized light is given by

$$A_H = (A_\alpha)_H + (A_\beta)_H + (A_u)_H, \quad (\text{A11})$$

while that for vertically polarized light is

$$A_V = (A_\alpha)_V + (A_\beta)_V + (A_u)_V. \quad (\text{A12})$$

These definitions are substituted in Eq. A6 to give

$$\begin{aligned} R - 1 &= \frac{A_V}{A_H} - 1 = \frac{A_V - A_H}{A_H} \\ &= \frac{(A_\alpha)_V - (A_\alpha)_H + (A_\beta)_V - (A_\beta)_H}{A_H} \\ &= \frac{(A_\alpha)_H}{A_H} \left[ \frac{(A_\alpha)_V}{(A_\alpha)_H} - 1 \right] + \frac{(A_\beta)_H}{A_H} \left[ \frac{(A_\beta)_V}{(A_\beta)_H} - 1 \right] \\ &= f'_\alpha (R'_\alpha - 1) + f'_\beta (R'_\beta - 1). \end{aligned} \quad (\text{A13})$$

The parameters  $f'_\alpha$  and  $f'_\beta$  are defined as

$$f'_\alpha = (A_\alpha)_H / A_H \quad (\text{A14})$$

$$f'_\beta = (A_\beta)_H / A_H. \quad (\text{A15})$$

That is, they are fractions of the absorption for horizontally polarized light due to the  $\alpha$ -helix and  $\beta$ -sheet, respectively.

To evaluate  $f'_\alpha$  and  $f'_\beta$ , we consider the absorbance of an isotropic sample of the same protein. This is given by

$$A_{\text{iso}} = ncl (f_\alpha \epsilon_\alpha + f_\beta \epsilon_\beta + f_u \epsilon_u), \quad (\text{A16})$$

where  $n$  is the number of residues in the protein;  $c$  is the molar concentration of the protein;  $l$  is the pathlength;  $f_\alpha$ ,  $f_\beta$ , and  $f_u$  are the fractions of the various types of secondary structure; and  $\epsilon_\alpha$ ,  $\epsilon_\beta$ , and  $\epsilon_u$  are the molar extinction coefficients, per residue, for the corresponding types of secondary structure at the frequency of interest. In the oriented sample, the  $\alpha$ -helix contribution to the absorbance for horizontally polarized light will be

$$(A_\alpha)_H = ncl f_\alpha \epsilon_\alpha (1 - S'_\alpha), \quad (\text{A17})$$

and that for the  $\beta$ -sheet will be

$$(A_\beta)_H = ncl f_\beta \epsilon_\beta (1 - S'_\beta). \quad (\text{A18})$$

Substituting Eqs. A17 and A18 into Eq. A14, we obtain the following expressions for  $f'_\alpha$  and  $f'_\beta$ :

$$f'_\alpha = \frac{f_\alpha \epsilon_\alpha (1 - S'_\alpha)}{f_\alpha \epsilon_\alpha (1 - S'_\alpha) + f_\beta \epsilon_\beta (1 - S'_\beta) + f_u \epsilon_u} \quad (\text{A19})$$

$$f'_\beta = \frac{f_\beta \epsilon_\beta (1 - S'_\beta)}{f_\alpha \epsilon_\alpha (1 - S'_\alpha) + f_\beta \epsilon_\beta (1 - S'_\beta) + f_u \epsilon_u} \quad (\text{A20})$$

Substitution of these equations, together with Eqs. A9 and A10 into Eq. A13 gives

$$R - 1 = 3 \sin^2 \theta \frac{f_\alpha \epsilon_\alpha S'_\alpha + f_\beta \epsilon_\beta S'_\beta}{f_\alpha \epsilon_\alpha (1 - S'_\alpha) + f_\beta \epsilon_\beta (1 - S'_\beta) + f_u \epsilon_u}. \quad (\text{A21})$$

It is useful to eliminate the extinction coefficient for the unordered form,  $\epsilon_u$ , by defining the relative extinction coefficients for the  $\alpha$ -helix and  $\beta$ -sheet:

$$\epsilon'_\alpha = \epsilon_\alpha / \epsilon_u \quad (\text{A22})$$

$$\epsilon'_\beta = \epsilon_\beta / \epsilon_u. \quad (\text{A23})$$

Substitution of these definitions in Eq. A21 leads to the following equation:

$$R - 1 = 3 \sin^2 \theta \frac{f_\alpha \epsilon'_\alpha S'_\alpha + f_\beta \epsilon'_\beta S'_\beta}{f_\alpha \epsilon'_\alpha (1 - S'_\alpha) + f_\beta \epsilon'_\beta (1 - S'_\beta) + f_u}. \quad (\text{A24})$$

We are grateful to Dr. Winslow S. Caughey for allowing us to use his IR spectrophotometers; to Dr. Lawrence J. Young for instruction and assistance in the initial preparation of cytochrome oxidase; to Drs. Kenneth J. Rothschild and Noel Clark for their assistance in our acquisition and initial use of the isopotential spin-drying apparatus; to Dr. Jen Tsi Yang for providing his basis spectra for CD analysis; and to Dr. Stephen Provencher for providing a copy of his program, CONTIN.

This work was supported by a grant from the U.S. Public Health Service, GM 22994.

Received for publication 16 May 1985 and in final form 29 July 1985.

## REFERENCES

1. Caughey, W. S., W. J. Wallace, J. A. Volpe, and S. Yoshikawa. 1976. Cytochrome *c* oxidase. In *The Enzymes*. P. D. Boyer, editor. Academic Press Inc., New York. 13:299-344.
2. Wikstrom, M., K. Krab, and M. Saraste. 1981. Cytochrome Oxidase: A Synthesis. Academic Press Inc., Ltd., London.
3. Capaldi, R. A., F. Malatesta, and V. M. Darley-Usmar. 1983. Structure of cytochrome oxidase. *Biochim. Biophys. Acta*. 726:135-148.
4. Deatherage, J. F., R. Henderson, and R. A. Capaldi. 1982. Three-dimensional structure of cytochrome *c* oxidase vesicle crystals in negative stain. *J. Mol. Biol.* 158:487-499.
5. Deatherage, J. F., R. Henderson, and R. A. Capaldi. 1982. Relationship between membrane and cytoplasmic domains of cytochrome *c* oxidase by electron microscopy in media of different density. *J. Mol. Biol.* 158:501-514.
6. Blasic, J. K., M. Erecinska, S. Samuels, and J. S. Leigh, Jr. 1978. The structure of a cytochrome oxidase-lipid model membrane. *Biochim. Biophys. Acta*. 501:33-52.



7. Azzi, A. 1980. Cytochrome *c* oxidase. Towards a clarification of its structure, interactions and mechanism. *Biochim. Biophys. Acta*. 594:231–252.
8. Kadenbach, B., and P. Merle. 1981. On the function of multiple subunits of cytochrome *c* oxidase from higher eukaryotes. *FEBS (Fed. Eur. Biochem. Soc.) Lett.* 135:1–11.
9. Capaldi, R. A. 1982. Arrangement of proteins in the mitochondrial inner membrane. *Biochim. Biophys. Acta*. 694:291–306.
10. Tanaka, M., M. Haniu, K. T. Yasunobu, C. A. Yu, L. Yu, Y. H. Wei, and T. E. King. 1977. Amino acid sequence of the heme *a* subunit of bovine heart cytochrome oxidase and sequence homology with myoglobin. *Biochem. Biophys. Res. Commun.* 76:1014–1019.
11. Anderson, S., A. T. Bankier, B. G. Barrell, M. H. L. de Bruijn, A. R. Coulson, J. Drouin, I.-C. Eperon, D. P. Nierlick, B. A. Roe, F. Sanger, P. H. Schreier, A. J. H. Smith, R. Staden, and I. G. Young. 1981. Sequence and organization of the human mitochondrial genome. *Nature (Lond.)*. 290:457–465.
12. Buse, G., G. J. Steffens, G. C. M. Steffens, R. Sacher, and M. Erdweg. 1982. Primary structure and function of cytochrome *c* oxidase subunits. In *Electron Transport and Oxygen Utilization*. C. Ho, editor. Elsevier-North Holland, New York. 157–163.
13. Senior, A. E. 1983. Secondary and tertiary structure of membrane proteins involved in proton translocation. *Biochim. Biophys. Acta*. 726:81–95.
14. Muccio, D. D., and J. Y. Cassim. 1979. Interpretation of the absorption and circular dichroic spectra of oriented purple membrane films. *Biophys. J.* 26:427–440.
15. Rothschild, K. J., and N. A. Clark. 1979. Polarized infrared spectroscopy of oriented purple membrane. *Biophys. J.* 25:473–488.
16. Nabedryk, E., and J. Breton. 1981. Orientation of intrinsic proteins in photosynthetic membranes. Polarized infrared spectroscopy of chloroplasts and chromatophores. *Biochim. Biophys. Acta*. 635:515–524.
17. Rothschild, K. J., N. A. Clark, K. M. Rosen, R. Sanches, and T. L. Hsiao. 1980. Spectroscopic studies of photoreceptor membrane incorporated into a multilamellar film. *Biochem. Biophys. Res. Commun.* 92:1266–1272.
18. Rothschild, K. J., R. Sanches, T. L. Hsiao, and N. A. Clark. 1980. Spectroscopic study of rhodopsin  $\alpha$ -helix orientation. *Biophys. J.* 31:53–64.
19. Nabedryk, E., D. M. Tiede, P. L. Dutton, and J. Breton. 1982. Conformation and orientation of the protein in the bacterial photosynthetic reaction center. *Biochim. Biophys. Acta*. 682:273–280.
20. Nabedryk, E., S. Andrianambintsoa, and J. Breton. 1984. Transmembrane orientation of  $\alpha$ -helices in the thylakoid membrane and in the light-harvesting complex. A polarized infrared spectroscopy study. *Biochim. Biophys. Acta*. 765:380–387.
21. Breton, J., and E. Nabedryk. 1984. Transmembrane orientation of  $\alpha$ -helices and the organization of chlorophyll in photosynthetic pigment-protein complexes. *FEBS (Fed. Eur. Biochem. Soc.) Lett.* 176:355–359.
22. Yoshikawa, S., M. G. Choc, M. C. O'Toole, and W. S. Caughey. 1977. An infrared study of CO binding to heart cytochrome *c* oxidase and hemoglobin A. Implications *re* O<sub>2</sub> reactions. *J. Biol. Chem.* 252:5498–5508.
23. van Gelder, B. F., and E. C. Slater. 1963. Titration of cytochrome *c* oxidase with NADH and phenazine methosulfate. *Biochim. Biophys. Acta*. 73:663–665.
24. Clark, N. A., K. J. Rothschild, D. A. Luippold, and B. A. Simon. 1980. Surface-induced lamellar orientation of multilayer membrane arrays. Theoretical analysis and a new method with application to purple membrane fragments. *Biophys. J.* 31:65–96.
25. Chen, G. C., and J. T. Yang. 1977. Two-point calibration of circular dichrometer with d-10-camphorsulphonic acid. *Anal. Lett.* 10:1195–1207.
26. Myer, Y. P. 1971. Conformation of cytochromes. V. Cytochrome *c* oxidase. *J. Biol. Chem.* 246:1241–1248.
27. Savitzky, A., and M. J. E. Golay. 1964. Smoothing and differentiation of data by simplified least squares procedures. *Anal. Chem.* 36:1627–1639.
28. Levenberg, K. 1944. A method for the solution of certain non-linear problems in least squares. *Q. Appl. Math.* 2:164–168.
29. Urry, D. W. 1972. Protein conformation in biomembranes: optical rotation and absorption of membrane suspensions. *Biochim. Biophys. Acta*. 265:115–168.
30. Tinoco, I., Jr., M. F. Maestre, and C. Bustamante. 1980. The optical activity of nucleic acids and their aggregates. *Annu. Rev. Biophys. Bioeng.* 9:107–114.
31. Tinoco, I., Jr., M. F. Maestre, and C. Bustamante. 1983. Circular dichroism in samples which scatter light. *Trends Biochem. Sci.* 8:41–44.
32. Bolotina, I. A., V. O. Chekhov, V. Y. Lugauskas, and O. B. Ptitsyn. 1980. Determination of the secondary structure of proteins from the circular dichroism spectra. II. Consideration of the contribution of  $\beta$ -bends. *Mol. Biol. (Engl. Transl. Mol. Biol. [Mosc.])* 14:709–715.
33. Bolotina, I. A., V. O. Chekhov, V. Y. Lugauskas, and O. B. Ptitsyn. 1981. Determination of the secondary structure of proteins from the circular dichroism spectra. III. Protein-derived reference spectra for antiparallel and parallel  $\beta$ -structures. *Mol. Biol. (Engl. Transl. Mol. Biol. [Mosc.])* 15:130–137.
34. Chang, C. T., C. S. Wu, and J. T. Yang. 1978. Circular dichroic analysis of protein conformation: inclusion of the  $\beta$ -turns. *Anal. Biochem.* 92:13–31.
35. Hennessey, J. P., Jr., and W. C. Johnson, Jr. 1981. Information content in the circular dichroism of proteins. *Biochemistry*. 20:1085–1094.
36. Provencher, S. W., and J. Glöckner. 1981. Estimation of globular protein secondary structure from circular dichroism. *Biochemistry*. 20:33–37.
37. Draper, N. R., and R. C. van Nostrand. 1979. Ridge regression and James-Stein estimation: review and comments. *Technometrics*. 21:451–466.
38. Bazzi, M. D. 1984. Orientation of cytochrome oxidase, Ca<sup>2+</sup>-ATPase, and poly(Leu-Lys) in membranes: a CD and IR study. Ph.D. thesis, Colorado State University. 173–186.
39. Michel-Villaz, M., H. R. Saibil, and M. Chabre. 1979. Orientation of rhodopsin  $\alpha$ -helices in retinal rod outer segment membranes studied by infrared linear dichroism. *Proc. Natl. Acad. Sci. USA*. 76:4405–4408.
40. Rothschild, K. J., K. M. Rosen, and N. A. Clark. 1980. Incorporation of photoreceptor membrane into a multilamellar film. *Biophys. J.* 31:45–52.
41. Heyn, M. P., R. J. Cherry, and U. Miller. 1977. Transient and linear dichroism studies on bacteriorhodopsin: determination of the orientation of the 568 nm all-trans retinal chromophore. *J. Mol. Biol.* 117:607–620.
42. Tsuboi, M. 1962. Infrared dichroism and molecular conformation of the  $\alpha$  form of poly( $\gamma$ -benzyl-L-glutamate). *J. Polym. Sci. Part D. Macromol. Rev.* 59:139–153.
43. Suzuki, E. 1971. (As quoted by R. D. B. Fraser and T. P. MacRae 1973.) Conformation in Fibrous Proteins and Related Synthetic Polypeptides. Academic Press, Inc., New York. 207–209.
44. Moffitt, W. 1956. Optical rotatory dispersion of helical polymers. *J. Chem. Phys.* 25:467–478.
45. Woody, R. W., and I. Tinoco, Jr. 1967. Optical rotation of oriented helices. III. Calculation of the optical rotatory dispersion and circular dichroism of the  $\alpha$ - and  $3_{10}$ -helix. *J. Chem. Phys.* 46:4927–4945.
46. Mandel, R., and G. Holzwarth. 1972. Circular dichroism of oriented helical polypeptides: the  $\alpha$ -helix. *J. Chem. Phys.* 57:3469–3477.

47. Kawai, M., and G. D. Fasman. 1978. A model  $\beta$ -turn. Circular dichroism and infrared spectra of a tripeptide. *J. Am. Chem. Soc.* 100:3630-3632.
48. Bandekar, J., and S. Krimm. 1979. Vibrational analysis of peptides, polypeptides, and proteins: characteristic amide bands of  $\beta$ -turns. *Proc. Natl. Acad. Sci. USA.* 76:774-777.
49. Myer, Y. P. 1970. A new method for the conformational analysis of proteins and polypeptides from circular dichroism spectra. *Res. Commun. Chem. Pathol. Pharmacol.* 1:607-616.
50. Capaldi, R. A. 1973. A hydrogen-deuterium exchange study of membranous cytochrome oxidase. *Biochim. Biophys. Acta.* 303:237-241.
51. Smith, J. C., and R. W. Woody. 1973. Optical and other properties of a hydrocarbon-soluble polypeptide, poly- $\gamma$ -(*n*-dodecyl)-L-glutamate. *Biopolymers.* 12:2657-2665.
52. Woody, R. W. 1977. Optical rotatory properties of biopolymers. *J. Polym. Sci. Part D. Macromol. Rev.* 12:181-321.
53. Miyazawa, T., and E. R. Blout. 1961. The infrared spectra of polypeptides in various conformations: amide I and II bands. *J. Am. Chem. Soc.* 83:712-719.
54. Fraser, R. D. B., and T. P. MacRae. 1973. *Conformation in Fibrous Proteins and Related Synthetic Polypeptides.* Academic Press, Inc., New York. 205-209.
55. Bradbury, E. M., L. Brown, A. R. Downie, A. Elliott, R. D. B. Fraser, and W. E. Hanby. 1962. The structure of the  $\omega$ -form of poly- $\beta$ -benzyl-L-aspartate. *J. Mol. Biol.* 5:230-247.
56. Henderson, R., and P. N. T. Unwin. 1975. Three-dimensional model of purple membrane obtained by electron microscopy. *Nature (Lond.)* 257:28-32.
57. Leifer, D., and R. Henderson. 1983. Three-dimensional structure of orthorhombic purple membrane at 6.5Å resolution. *J. Mol. Biol.* 163:451-466.
58. Rothschild, K. J., and N. A. Clark. 1979. Anomalous amide I infrared absorption of purple membrane. *Science (Wash. DC).* 204:311-312.
59. Krimm, S., and A. M. Dwivedi. 1982. Infrared spectrum of the purple membrane: clue to a proton conduction mechanism? *Science (Wash. DC).* 216:407-408.
60. Némethy, G., D. C. Phillips, S. J. Leach, and H. A. Scheraga. 1967. A second right-handed helical structure with the parameters of the Pauling-Corey  $\alpha$ -helix. *Nature (Lond.)* 214:363-365.
61. Phillips, W. C., D. L. D. Caspar, R. Saper, and D. A. Goodenough. 1985.  $\beta$ -Sheet conformation in the gap junction connexon protein. *Biophys. J.* 47(2, Pt. 2):252a (Abstr.)
62. Rosenbusch, J. P. 1974. Characterization of the major envelope protein from *Escherichia coli*. Regular arrangement of the peptidoglycan and unusual dodecyl sulfate binding. *J. Biol. Chem.* 249:8019-8029.
63. Jap, B. K., M. F. Maestre, S. B. Hayward, and R. M. Glaeser. 1983. Peptide-chain secondary structure of bacteriorhodopsin. *Biophys. J.* 43:81-89.